# Thermally Stable Luminescent Composites Fabricated by Confining Rare Earth Complexes in the Two-Dimensional Gallery of Titania Nanosheets and Their Photophysical Properties

**Hao Xin, Yasuo Ebina, Renzhi Ma, Kazunori Takada, and Takayoshi Sasaki***

*Nanoscale Materials Center, National Institute for Materials Science, 1−1 Namiki, Tsukuba, Ibaraki 305-0044, Japan*

*Received: March 8, 2006*

Fluorescent composite materials of exfoliated titania nanosheets, $Ti_{0.91}O_2$, and rare earth (RE) complexes, $Eu(phen)_2Cl_3 \cdot 2H_2O$ and $Tb(phen)_2Cl_3 \cdot 2H_2O$ (phen = 1,10-phenanthroline), were synthesized via flocculation between them. X-ray diffraction measurements and transmission electron microscopy observations confirmed a restacked lamellar structure for the composites, and elemental analysis revealed a high RE complex content of 15 wt %. The decomposition temperature of the complexes trapped in the composites was improved to 420 °C from 250 °C for the free form. The restacked composite composed of $Ti_{0.91}O_2$ nanosheets and $Eu(phen)_2$ exhibited characteristic red emission from the complex, while the composite with $Tb(phen)_2$ gave featureless emission originated from the ligand. This phenomenon can be explained by a shift of triplet state level of the ligand after encapsulation in the host titania nanosheets. The quantum yield of europium complex in the composite was enhanced 1.6 times more than that of the pure complex.

## Introduction

Rare earth (RE) or lanthanide (Ln) complexes, particularly those with ligands such as $\beta$-diketone, aromatic carboxylic acid, and phenanthroline, have excellent photoluminescence (PL) characteristics, which originate in strong optical absorption in the ultraviolet region by the ligands and the effective energy transfer from the ligands to central RE ions. Thus, these complexes have attracted significant interest in technological applications including optoelectronic devices and flat panel displays.[1−3] Unfortunately, however, RE complexes must be incorporated into stable rigid matrixes for practical applications due to their poor thermal stability. One of the methods most studied is the sol−gel approach,[4−14] through which RE complexes are introduced into a matrix of polymer or silica gel. Such composite materials showed improved thermal stability and mechanical properties of the complexes, keeping good luminescence properties. However, the following problems still limit their practical use. First, a doping concentration of the complexes is very limited because of their poor solubility into the matrices. Second, the complexes tend to aggregate in the matrices and their homogeneous dispersion is difficult to achieve.

To overcome these drawbacks, several groups have proposed the encapsulation of RE complexes into inorganic hosts, such as zeolite Y[15] and zirconium phosphate ($\alpha$-ZrP).[16] Some pretreatment of the host materials is needed because of difficulties in direct incorporation of complexes into these host materials. For example, the interlayer gallery of $\alpha$-ZrP was preswollen by intercalation of *p*-methoxyaniline, to which RE complexes were introduced by ion-exchange reactions. However, only a small amount of the preintercalated organic species could be driven out by the complexes and, consequently, the loading of RE complexes was still low.[16]

Recently, we have successfully synthesized fluorescent materials by restacking exfoliated titania nanosheets of $Ti_{0.91}O_2^{0.36-}$ with RE ions themselves (Eu and Tb).[17] Thanks to this synthetic route, the composites had a homogeneous layered structure accommodating the RE ions between titania nanosheets with a high content (10 ± 1 mol %). Energy transfer was observed between titania nanosheets and Eu(III) ions, leading to characteristic Eu(III) emission both by exciting Eu(III) ions and the host titania nanosheets. However, this energy transfer in the composite was not as efficient as that from organic ligands to RE ions in the complexes, resulting in relatively low emission intensity. Here we report on new luminescent composites in which RE complexes ($Eu(phen)_2Cl_3 \cdot 2H_2O$ and $Tb(phen)_2Cl_3 \cdot 2H_2O$, phen = 1,10-phenanthroline) are encapsulated between inorganic nanosheets by the restacking method.

## Experimental Section

The unilamellar titania nanosheet, $Ti_{0.91}O_2$, was synthesized by delaminating a layered protonic oxide of $H_{0.7}Ti_{1.825}O_4 \cdot H_2O$ through the procedures described in our previous reports.[18,19] RE complexes, $Ln(phen)_2Cl_3 \cdot 2H_2O$, were synthesized according to the literature.[20] The composite was prepared by the slow addition of a complex solution (0.1 mol $dm^{-3}$ in DMF) to the colloidal suspension of $Ti_{0.91}O_2$ nanosheets (100 $cm^3$, pH = 6.8, 0.2 wt %) under stirring at room temperature until the nanosheets were completely flocculated. The precipitated product was filtered, washed with ultrapure water, and dried in air. The two composites are expressed as ex-$Ti_{0.91}O_2$/$Eu(phen)_2$ and ex-$Ti_{0.91}O_2$/$Tb(phen)_2$, respectively, where "ex-" means "exfoliated". Composites of ex-$Ti_{0.91}O_2$/PDDA and ex-$Ti_{0.91}O_2$/H were prepared in a similar procedure using poly(diallyldimethylammonium chloride) (PDDA) and HCl as the flocculating agents.[21]

X-ray diffraction (XRD) patterns were collected using a Rigaku Rint 2000S powder diffractometer with graphite monochromatized Cu K$\alpha$ radiation ($\lambda$ = 0.15405 nm). Thermogravimetric analysis (TGA) measurements were carried out under an Ar gas flow at a heating rate of 3 °C $min^{-1}$ on a Rigaku TG 8120 thermal analyzer. UV−vis absorption spectra were recorded in the diffuse reflectance mode on a Hitachi U-4000

* Corresponding author. Phone: +81-29-860-4313. Fax: +81-29-854-9061. E-mail: sasaki.takayoshi@nims.go.jp.

10.1021/jp061427g CCC: $33.50 © 2006 American Chemical Society
Published on Web 04/29/2006

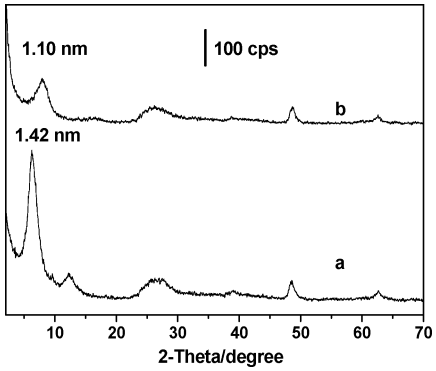


**Figure 1.** XRD patterns of ex-$Ti_{0.91}O_2$/Eu(phen)$_2$ (a) and its heat-treated sample (400 °C for 1 h) (b).

spectrophotometer. FT−IR spectra were measured on a sample pelleted with KBr with a Digilab S-45 FT−IR spectrometer equipped with liquid nitrogen cooled MCT detector. Transmission electron microscopy (TEM) observations were performed using a high-resolution TEM microscope (JEM-3000F) with energy-dispersive X-ray spectrometer (EDS).

Room-temperature PL excitation and emission spectra were obtained on a Hitachi F-4500 fluorescence spectrophotometer. Phosphorescence spectra were acquired using the 325-nm light from a cw He−Cd laser, and the excitation power density was around 0.1 $Wcm^{-2}$. The samples were mounted in the coldfinger of a closed-cycle helium cryostat. The luminescence was measured using a Spex 1704 monochromator (1 m, 1200 $mm^{-1}$) equipped with a CCD detector. The spectra were corrected for the wavelength response of the optical system. The quantum yield was measured using an integrating sphere on a MCPD-7000 High Sensitivity Spectra Multiphoto Detector (Tsuka Electronics). A 150 W Xe lamp was used as the source light.

## Results and Discussion

**Materials Synthesis.** Colloidal titania nanosheets were synthesized by exfoliating a protonic layered titanate, $H_{0.7}Ti_{1.825}O_4 \cdot H_2O$, into single layers, which is achieved by the reaction with tetrabutylammonium (TBA) ions.[18,19] Composites were synthesized by slow addition of a RE complex solution (dissolved in DMF) to the nanosheet aqueous suspension under stirring at room temperature. A precipitate with a wool-like appearance was slowly formed. The resulting two samples (ex-$Ti_{0.91}O_2$/Eu(phen)$_2$ and ex-$Ti_{0.91}O_2$/Tb(phen)$_2$) showed very similar compositional and structural characteristics due to the nearly identical chemical nature and molecular structure of the complexes. Elemental analysis on ex-$Ti_{0.91}O_2$/Eu(phen)$_2$ indicated its chemical composition as $H_{0.25}[Eu(phen)_2]_{0.03}(TBA)_{0.01}Ti_{0.91}O_2 \cdot 0.5H_2O$ (Found: Ti, 42.1%; Eu, 4.3%; C, 11.1%; N, 1.7%. Calcd.: Ti, 42.4%; Eu, 4.4%; C, 10.3%; N, 1.8%.). It should be noted that the complex content corresponds to about 15 wt % of the composite, which is much higher than previous results with other hosts, e.g., α-ZrP. The observed contents for C and N were slightly larger than the values expected from the chemical formula of Eu(phen)$_2$. We attributed these excess C and N to TBA ions coprecipitated upon flocculation. In fact, Fourier Transform Infrared (FT−IR) spectroscopy measurements detected absorption bands attributable to TBA ions, as will be described below. We assume that the charge is balanced with protons as well. This may be due to the so-called covering effect and will be discussed below.

**Characterizations.** Figure 1a shows the XRD pattern of as-prepared composite of ex-$Ti_{0.91}O_2$/Eu(phen)$_2$. Two peaks at a $2\theta$ value of 48.5° and 62.6° are attributable to the two-dimensional atomic arrangement in $Ti_{0.91}O_2$ nanosheet.[18] The basal diffraction peaks at $2\theta = 6.2°$ and 12.4° indicate a layered structure with a gallery height of 1.42 nm. Transmission electron microscope (TEM) images in Figure 2 further confirmed the lamellar nature of the material, showing a clear fringe with a spacing of 1.4−1.5 nm.

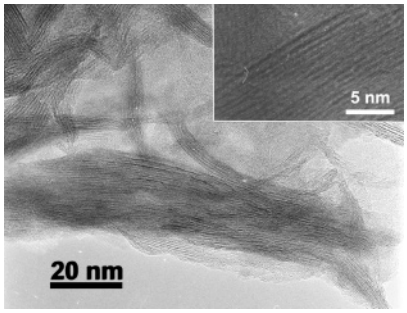


**Figure 2.** TEM images of composite ex-$Ti_{0.91}O_2$/Eu(phen)$_2$.

The low-temperature PL spectrum (See Supporting Information) revealed that the complex En(phen)$_3$Cl$_3$·H$_2$O adopts a trans-structure. Four nitrogen atoms are equatorially coordinated to $Eu^{3+}$ ion while one water molecule and one chloride ion are vertically coordinated. This configuration is compatible with F. A. Hart's proposal.[22] The lateral dimension of the complex ion Eu(phen)$_2$ can be roughly calculated to be 1.49 × 1.14 $nm^2$ (see Supporting Information, Figure S3). On the other hand, the nanosheet has a two-dimensional unit cell of 0.30 × 0.38 $nm^2$, in which two formulas of $Ti_{0.91}O_2$ are included.[25] If the planar complex is assumed to be accommodated as a close-packed monolayer in parallel orientation to the nanosheets, one complex covers the gallery area which corresponds to approximately 15 ( =(1.49 × 1.14)/(0.30 × 0.38)) unit cells of the nanosheet. Based on this model, the complex content is expected to be 0.03 ( =1/(15 × 2)), which is in excellent agreement with the observed composition. Two plus charges for one complex are too small to compensate for the minus charges of the nanosheet in the corresponding area.

The gallery height of 1.42 nm can be understood in terms of the sum of the nanosheet thickness (∼0.75 nm),[23,24] the thickness of the aromatic rings of the complex (∼0.34 nm), and the size of water molecules (∼0.3 nm). The water content, 0.5 per chemical formula, indicates one water molecule per unit-cell area of the nanosheet, which is large enough to form a monolayer by itself in the nanosheet gallery.

Upon heat treatment at 400 °C, the gallery height shrank to 1.1 nm (Figure 1b). The intersheet shrinkage of ∼0.3 nm is close to the size of water molecules. This suggests that the complexes in the nanosheet gallery were preserved at 400 °C, the only change being the dehydration.

Figure 3 compares FT−IR spectra of the as-flocculated composite of ex-$Ti_{0.91}O_2$/Eu(phen)$_2$ and its sample heat treated at 400 °C for 1h with that of the complex Eu(phen)$_2$Cl$_3$·2H$_2$O itself. The as-flocculated sample exhibited rather broad absorption bands in a wavelength range of 3700−3000, ∼1630, 1000−400 $cm^{-1}$, which are attributable to stretching and bending modes of water molecules and vibrational modes of Ti−O bonds, respectively. Additionally, many sharp absorption bands were observed overlapped with the broad features. Most of them were superimposable on the spectral features of the complex itself, clearly supporting its successful encapsulation. There were several peaks (indicated by numbers in Figure 3b) which cannot be ascribed to the complex. These may be explained by the presence of TBA ions,[25] which is also suggested from the chemical analysis data and the structure consideration above.

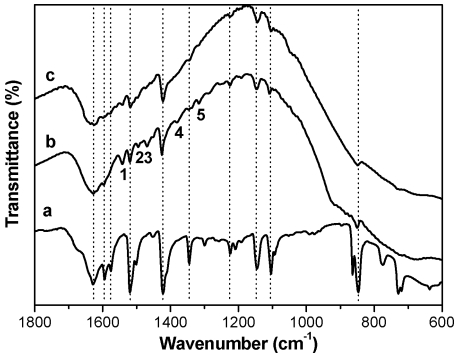


**Figure 3.** FT−IR spectra of $Eu(phen)_2Cl_3 \cdot 2H_2O$ (a), ex-$Ti_{0.91}O_2$/$Eu(phen)_2$ (b) and ex-$Ti_{0.91}O_2$/$Eu(phen)_2$ heat treated at 400 °C (c). Dotted lines indicate the location of the prominent absorption bands from the complex. Peak wavenumbers indicated by numbers: 1, 1542 $cm^{-1}$; 2, 1495 $cm^{-1}$; 3, 1469 $cm^{-1}$; 4, 1381 $cm^{-1}$; 5, 1316 $cm^{-1}$.

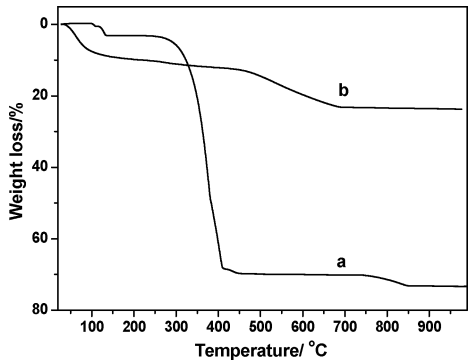


**Figure 4.** TGA curves of the complex, $Eu(phen)_2Cl_3 \cdot 2H_2O$, (a) and composite, ex-$Ti_{0.91}O_2$/$Eu(phen)_2$ (b).

Interestingly, these peaks disappeared upon heating at 400 °C, while those from the complex remained unchanged. This strongly suggests that the complex in the nanosheet gallery survived at 400 °C where TBA ions were combusted.

The thermal analysis provided direct evidence for the improved thermal stability of the complex between the nanosheets. The data of the free complex, $Eu(phen)_2Cl_3 \cdot 2H_2O$, and the composite, ex-$Ti_{0.91}O_2$/$Eu(phen)_2$ are compared in Figure 4. The complex itself lost a weight of 3.1% at temperatures up to 150 °C due to the evaporation of one crystal water per formula weight (calcd 2.8% cal). Another water molecule was not evaporated, suggesting tight coordination to the metal ion. The steep and large weight loss that started at 250 °C should be ascribed to the decomposition of the organic ligand. On the other hand, the composite underwent dehydration up to 150 °C, giving a weight loss of 9.1%. This is consistent with the value of 8.7% expected from the chemical formula above. A slight and gradual weight loss in a temperature range of 200−300 °C may be attributed to the removal of TBA ions. The observed loss of 2.1% roughly agrees with the expected amount of 2.4%. There was another weight loss of 11.6% above 420 °C. This weight loss may involve the combustion of the ligand and the deliberation of the protons as $H_2O$ molecules. These thermal events are expected to yield the losses of 10.5% and 2.2%, respectively, from the chemical formula.

The marked improvement in thermal stability by the confinement of the complex in the inorganic host is consistent with XRD (Figure 1) and FT−IR (Figure 3) results. The higher stability may be the result of supplemental interaction between the negatively charged titania nanosheets and RE complex ions.

Figure 5 depicts UV−vis absorption spectra for the composite samples of ex-$Ti_{0.91}O_2$/$Ln(phen)_2$ and the free complexes. In addition to these, $Ti_{0.91}O_2$ nanosheets were restacked using a HCl solution (0.1 mol $dm^{-3}$) as a flocculating agent, and its data is also included for comparison. The complexes showed a huge absorption in a wavelength range of 200−400 nm, which is associated with $\pi - \pi^*$ transitions in the aromatic ligands. In addition, small sharp peaks were observed at 395, 418, 465, and 535 nm for $Eu(phen)_2Cl_3 \cdot 2H_2O$ (Figure 5a, indicated by circles), which are due to the intraconfigurational $4f-4f$ transitions of Eu (III) ions. On the other hand, the absorption of Tb ions was overlapped by that of ligand and no sharp peaks were detected. The nanosheets flocculated with acid, ex-$Ti_{0.91}O_2$/H, exhibited a strong band-gap absorption ($\lambda < 380$ nm) based on the semiconducting nature of the nanosheet. The composites, ex-$Ti_{0.91}O_2$/$Ln(phen)_2$, also had a strong absorption in the UV−vis region, which should be a combination of absorption by ligands of the complexes and the titania host. One of the most notable features is a small but significant red-shift in absorption compared with the free complexes. This suggests a reduction in the energy involving $\pi-\pi^*$ transitions in the ligands, which should be the result of the encapsulation of the complex between nanosheets. In the free complex, the charge distribution on both sides of the ligand plane may be different because the vertically coordinated chloride ion is negatively charged while the water molecule is neutral. This may bring about the decrease of the conjugation level of the ligand. In the composite, on the contrary, the complex is sandwiched by the negatively charged titania nanosheets, the charge distribution should be more symmetric than that in the free complex. This may enhance the conjugation level of the ligand and lead to the red-shifted absorption. In the case of α-ZrP[16] and silica[10] as hosts, in contrast, the RE complexes showed blue-shifted absorption. This might be caused by the distortion of ligands by surrounding hosts, resulting in the reduction of the stabilization of $\pi$ orbitals.

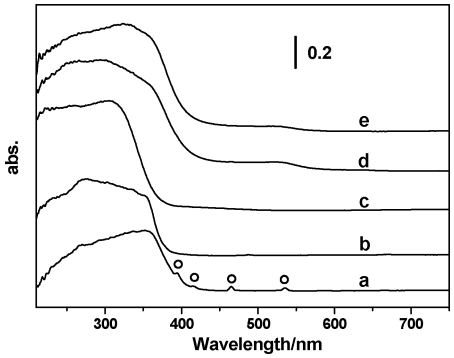


**Figure 5.** UV−vis absorption spectra of $Eu(phen)_2Cl_3 \cdot 2H_2O$ (a), $Tb(phen)_2Cl_3 \cdot 2H_2O$ (b), ex-$Ti_{0.91}O_2$/H (c), ex-$Ti_{0.91}O_2$/$Eu(phen)_2$ (d) and ex-$Ti_{0.91}O_2$/$Tb(phen)_2$ (e). The small sharp peaks due to $4f - 4f$ transitions of Eu ions in $Eu(phen)_2Cl_3 \cdot 2H_2O$ are indicated by circles.

The red-shifted absorption in ex-$Ti_{0.91}O_2$/$Eu(phen)_2$ is important for practical applications. Our experiments strongly suggested that a major fraction of the light with a wavelength of <350 nm is absorbed by $Ti_{0.91}O_2$ nanosheet, attenuating the irradiation to the species encapsulated between them.[17] The red-shift contributes to the alleviation of the overlap of the absorption by the complex and the host.

**Photophysical Properties.** Figure 6 shows PL spectra (both excitation and emission) of ex-$Ti_{0.91}O_2$/$Eu(phen)_2$ and $Eu(phen)_2Cl_3 \cdot 2H_2O$, ex-$Ti_{0.91}O_2$/$Tb(phen)_2$ and $Tb(phen)_2Cl_3 \cdot 2H_2O$. Each pair was recorded under identical conditions at room temperature. The excitation spectra of the free complexes had a profile very similar to their UV−vis absorption feature, indicating that the emission originates from the energy absorbed by the ligand. The small sharp peaks at 395, 418, and 465 nm

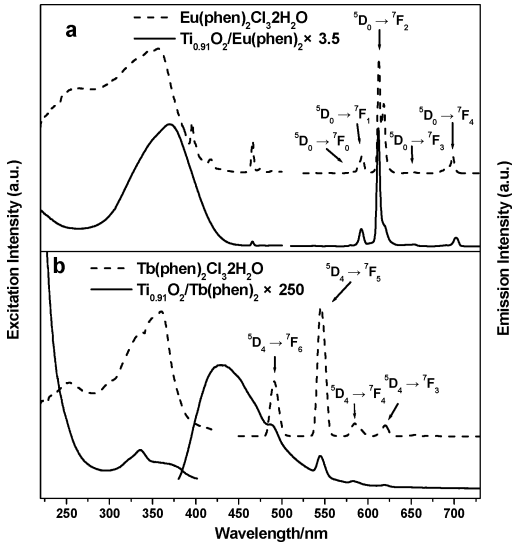


**Figure 6.** PL excitation and emission spectra of $Eu(phen)_2Cl_3 \cdot 2H_2O$ and ex-$Ti_{0.91}O_2$/$Eu(phen)_2$ (a), and $Tb(phen)_2Cl_3 \cdot 2H_2O$ and ex-$Ti_{0.91}O_2$/$Tb(phen)_2$ (b). The spectra were plotted in multiple scales for comparison. The excitation spectra were measured by monitoring the emission peak wavelength at 612 nm for $Eu(phen)_2Cl_3 \cdot 2H_2O$ and ex-$Ti_{0.91}O_2$/$Eu(phen)_2$, and 545 nm for $Tb(phen)_2Cl_3 \cdot 2H_2O$ and ex-$Ti_{0.91}O_2$/$Tb(phen)_2$, respectively. The emission spectra were measured under peak excitation light.

in the excitation spectrum of complex $Eu(phen)_2Cl_3 \cdot 2H_2O$ are due to the intraconfigurational $4f \rightarrow 4f$ transition of central Eu (III) ions. The five prominent emission peaks at 579, 593, 612, 650, and 698 nm for $Eu(phen)_2Cl_3 \cdot 2H_2O$ (Figure 5a) can be attributed to $^5D_0 \rightarrow {}^7F_J$ ($J = 0-4$) transition with red emission for $J = 2$ as the dominant feature. On the other hand, the four main peaks of $Tb(phen)_2Cl_3 \cdot 2H_2O$ at 490, 544, 585, and 620 nm correspond to $^5D_4 \rightarrow {}^7F_J$ ($J = 6-3$) transitions, respectively.

The composite material of ex-$Ti_{0.91}O_2$/$Eu(phen)_2$ showed a similar excitation spectral feature as the complex $Eu(phen)_2Cl_3 \cdot 2H_2O$, indicating that the emission is mainly from energy absorbed by the ligand, not the titania host. The maximum excitation wavelength for the composite sample appeared at 370 nm, which was red-shifted from 356 nm for the free complex. This is in good agreement with the UV−vis data and in contrast to the behavior reported for the complex incorporated in matrices of the polymers, zeolite Y and α-ZrP. On the other hand, the composite of ex-$Ti_{0.91}O_2$/$Tb(phen)_2$ exhibited a broad and relatively weak emission with a maximum at 430 nm, overlapped with detectable line-like characteristic emissions of Tb ions (Figure 6b). Obviously, this featureless emission originates from the ligands, suggesting that the energy transfer from the ligands to Tb(III) ions did not take place efficiently.

It has been established that the energy transfer in RE complexes proceeds as follows:[26] the ligand is excited, initially, to the singlet state ($S_1$) by photon absorption, which is subsequently relaxed to the triplet state ($T_1$). Finally, energy transfer to RE central ions takes place. The ligand singlet position can be estimated by referencing to its absorption edge and the triplet energy level can be obtained by measuring the phosphorescence spectra of the isostructural La (or Gd, Lu) (III)-based compounds.[27] Figure 7 shows the emission spectra of sample $La(phen)_2Cl_3 \cdot H_2O$ and ex-$Ti_{0.91}O_2$/$La(phen)_2$ measured at 12 K. From Figures 5 and 7, the first excited singlet and triplet energy levels of the ligand in the free complex Ln-$(phen)_2Cl_3 \cdot H_2O$ and composite ex-$Ti_{0.91}O_2$/$Ln(phen)_2$ are estimated to be 26 320 $cm^{-1}$ (380 nm), 23 810 $cm^{-1}$ (420 nm), 24 390 $cm^{-1}$ (410 nm), and 19 160 $cm^{-1}$ (522 nm), respectively.

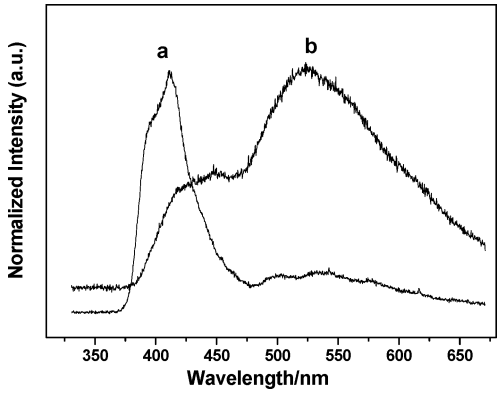


**Figure 7.** Phosphorescence spectra of $La(phen)_2Cl_3 \cdot 2H_2O$ (a) and ex-$Ti_{0.91}O_2$/$La(phen)_2$ at 12 K under 325 nm He−Cd laser excitation.

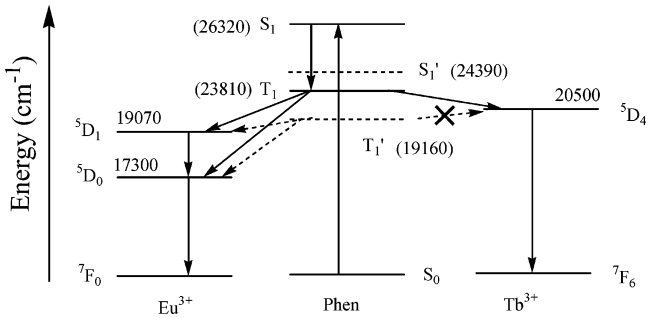


**Figure 8.** Schematic energy level diagram and the energy transfer process in the complex. $S_1$ and $T_1$: excited singlet and triplet state of the ligand in free complex; $S_1'$ and $T_1'$: excited singlet and triplet state of the ligand in composite.

The composite ex-$Ti_{0.91}O_2$/$La(phen)_2$ at 12 K showed an emission band peaked at 433 nm, the spectral feature of which is nearly the same as that measured at room temperature (not shown), is assigned to the fluorescence emission from the singlet state.[28]

Figure 8 illustrates the energy diagram on the basis of the data above. The ligand triplet state is higher than the $^5D_1$ and $^5D_0$ energy level of Eu(III) both in the complex $Eu(phen)_2Cl_3 \cdot H_2O$ and the composite ex-$Ti_{0.91}O_2$/$Eu(phen)_2$. Accordingly, energy absorbed by the ligand could be transferred to the central metal ions and the characteristic line-like emission was observed. These channels, through ground state→S→T→$^5D_1$→$^5D_0$→emission and ground state→S→T→$^5D_0$→emission, are the two most probable energy transfer routes due to their high transfer rates.[29] The emission property of the complex $Tb(phen)_2Cl_3 \cdot H_2O$ can be understood by the same mechanism. However, because the ligand triplet state in the composite ex-$Ti_{0.91}O_2$/$Tb(phen)_2$ is lower than Tb-(III) $^5D_4$ emissive level, energy transfer from the ligand to the metal ion cannot take place, leading to the direct relaxation of the exited singlet state of the ligand to its ground state and producing a weak fluorescence with a main peak at 430 nm.

**Estimation of Quantum Yield.** The emission quantum yield, $q$, light-absorption ratio, $\Delta_A$, and emission efficiency, $\eta$, were measured to quantitatively discuss the effects of the encapsulation on the luminescence performance. The $q$ value is defined as the ratio between the number of photons emitted by the Eu(III) ion and the number of photons absorbed by the ligands, while $\Delta_A$ is the ratio of the number of photons absorbed by the sample versus the incident number of photons. The emission efficiency equals to $q \times \Delta_A$. All measurements were carried out at room temperature using a compacted powder disk 2 mm thick to prevent insufficient absorption. Table 1 summarizes

**TABLE 1: Emission Quantum Yield, Absorption Ratio, and Emission Efficiency of Free Complex $Eu(phen)_2Cl_3 \cdot 2H_2O$, $Tb(phen)_2Cl_3 \cdot 2H_2O$, and Composite Ex-$Ti_{0.91}O_2$/$Eu(phen)_2$.[a]**

| sample | quantum yield ($q$) | absorption ratio ($\Delta_A$) | emission efficiency ($\eta$) |
|---|---|---|---|
| $Eu(phen)_2Cl_3 \cdot 2H_2O$[b] | 36.7% | 90.8% | 33.3% |
| $Tb(phen)_2Cl_3 \cdot 2H_2O$[b] | 12.2% | 90.9% | 11.1% |
| ex-$Ti_{0.91}O_2$/$Eu(phen)_2$[c] | 28.5%<br>60.2%[d] | 83.8% | 23.9% |
| ex-$Ti_{0.91}O_2$/PDDA[c] | | 44.1% | |

[a] The data were obtained at the peak excitation wavelength due to the ligand. The absorption ratio of ex-$Ti_{0.91}O_2$/PDDA is shown for comparison. [b] Excited at 356 nm. [c] Excited at 370 nm. [d] After excluding absorption of the host.

the results for different samples performed at their peak excitation wavelength. The complexes $Eu(phen)_2Cl_3 \cdot 2H_2O$ and $Tb(phen)_2Cl_3 \cdot 2H_2O$ show similar absorption ratio as expected due to their identical structure, but the quantum yield for terbium complex (12.2%) is much lower than that of europium complex (36.7%). This may be caused by a smaller energy difference (3310 $cm^{-1}$) between the ligand triplet state and the Tb(III) $^5D_4$ level, which may allow for the back energy transfer from the $^5D_4$ level to the excited ligand triplet state.[27,30]

The as-measured quantum yield and emission efficiency were 28.5% and 23.9%, respectively, for composite ex-$Ti_{0.91}O_2$/$Eu(phen)_2$, which are apparently lower than those for the free complex. However, this may not be intrinsic since the host titania nanosheet has absorption at the excitation wavelength, and this absorption does not contribute to complex emission as discussed above. To evaluate the magnitude of this absorption, PDDA was used as the flocculation agent instead of lanthanide complex to produce a composite ex-$Ti_{0.91}O_2$/PDDA. This composite has a lamellar structure with a gallery height of 1.4 nm similar to that of ex-$Ti_{0.91}O_2$/$Eu(phen)_2$. It may be reasonable to assume that the absorption by the titania nanosheet host in ex-$Ti_{0.91}O_2$/$Eu(phen)_2$ is similar to that in ex-$Ti_{0.91}O_2$/PDDA. Because PDDA has no absorption in a wavelength range of 200−800 nm,[20] and the absorption ratio of ex-$Ti_{0.91}O_2$/PDDA measured at 370 nm under the identical condition as ex-$Ti_{0.91}O_2$/$Eu(phen)_2$ was 44.1% (Table 1), the absolute absorption by the ligand could be roughly estimated to be 39.7% (=83.8−44.1). By taking into account the fact that the content of europium complex is 1/5.4 of that in the free complex, the ligand absorption coefficient in the composite is about 2.4 (=39.7/90.8 × 5.4) times higher than that in the free complex. This is confirmed by the excitation spectra in Figure 6. The ratio of the peak intensity from the ligand versus the intensity of the Eu(III) $f \rightarrow f$ transition at 465 nm is much higher in the composite than that in the free complex. The quantum yield of europium complex encapsulated between titania nanosheets can, therefore, be deduced to be 60.2% (=28.5 × 83.8/39.7), which is 1.6 times as large as that for the complex itself.

Moreover, when normalized by the complex content, the emission efficiency of the europium complex in the composite, $\eta$, is 3.8 (=23.9/33.3 × 5.4) times of that in the free complex, which is obviously the consequence of the improvement in absorption coefficient and quantum yield. The enhancement of the emission performance should benefit from the restacked lamellar structure. It is well-known that the excitation energy of the ligand can be lost by the vibration itself and the excitation energy of the Eu(III) ion can also be lost by the vibration of its nearest ligands (including water molecules). The rigid host structure of titania nanosheet may suppress the vibration of the ligand. More importantly, the encapsulation of the complex in the titania host lowered the triplet energy level of the ligand, leading to more efficient energy transfer. In addition, the complex molecules are homogeneously dispersed in the host, which makes the concentration quenching lower greatly.[31]

## Conclusions

We have demonstrated the synthesis of fluorescent composite materials of titania nanosheets and RE complexes for the first time by a simple flocculation method. The resulting composites had a homogeneous layered structure with a gallery height of 1.4 nm. The RE complexes were accommodated in the titania nanosheet host at a content as high as 15 wt %. The encapsulation resulted in the marked enhancement of the thermal stability and also significant modification of the photophysical properties of the lanthanide complexes. The singlet and triplet states of the ligand lowered upon incorporation between the nanosheets. This was confirmed by the red shift of UV−vis absorption and phosphorescence spectra measured on the isostructural lanthanum counterpart. The lowered ligand triplet state in the composite stays higher than the $^5D_1$ and $^5D_0$ energy levels of Eu(III) ion, but becomes lower than that the $^5D_4$ level of Tb(III) ions. As a result, the composite ex-$Ti_{0.91}O_2$/$Eu(phen)_2$ exhibited characteristic red emission from the europium complex, while ex-$Ti_{0.91}O_2$/$Tb(phen)_2$ only gave featureless emission originated from the ligand. The quantum yield of the europium complex in the composite is estimated to be 60.2%, which is 1.6 times that of the free complex. In addition, the unit emission efficiency is 3.8 times enhanced in the composite benefited from the improvement in absorption coefficient and quantum yield. These features suggest its potential for applications in optoelectronic devices. Our results indicate that incorporation of a rare earth emissive complex into a layered inorganic host material is a useful strategy to improve its thermal stability and emission efficiency.

**Acknowledgment.** The study has been supported by CREST of the Japan Science and Technology Agency (JST). We thank Dr. Rongjun Xie for quantum yield measurements, and we are grateful to Dr. Yuguang Wang and Dr. Yoshiki Wada for assistance in low-temperature luminescence measurements.

**Supporting Information Available:** Low-temperature luminescence spectra of $Eu(phen)_2Cl_3 \cdot 2H_2O$ and ex-$Ti_{0.91}O_2$/$Eu(phen)_2$, the scheme of complex $Ln(phen)_2Cl_3 \cdot 2H_2O$ and the estimated size of $Ln(phen)_3$ ion. This material is available free of charge via the Internet: http://pubs.acs.org.

## References and Notes

(1) Kido, J.; Okamoto, Y. *Chem. Rev.* **2002**, *102*, 2357.
(2) Xin, H.; Shi, M.; Zhang, X. M.; Li, F. Y.; Bian, Z. Q.; Ibrahim, K.; Liu, F. Q.; Huang, C. H. *Chem. Mater.* **2003**, *15*, 3728.
(3) Denning, R. G. *J. Mater. Chem.* **2001**, *11*, 19.
(4) Matthews, L.; Knobbe, E. T. *Chem. Mater.* **1993**, *5*, 1697.
(5) Yan, B.; Zhang, H. J.; Ni, J. Z. *Mater. Sci. Eng.* **1998**, *B52*, 123.
(6) Franville, A. C.; Zambon, D.; Mahiou, R.; Chou, S.; Troin, Y.; Cousseins, J. C. *J. Alloy. Compd.* **1998**, *277*, 831.
(7) Ji, X. L.; Li, B.; Jiang, S. C.; Dong, D. W.; Zhang, H. J.; Jing, X. B.; Jiang, B. Z. *J. Non-Cryst. Solids* **2000**, *275*, 52.
(8) Chuai, X. H.; Zhang, H. J.; Li, F. S.; Wang, S. B.; Zhou, G. Z. *Mater. Lett.* **2000**, *46*, 244.
(9) Franville, A. C.; Zambon, D.; Mahiou, R.; Troin, Y. *Chem. Mater.* **2000**, *12*, 428.
(10) Fu, L. S.; Xu, Q. H.; Zhang, H. J.; Li, L. S.; Meng, Q. G.; Xu, R. R. *Mater. Sci. Eng.* **2002**, *B88*, 68.
(11) Dong, D. W.; Jiang, S. C.; Men, Y. F.; Ji, X. L.; Jiang, B. Z. *Adv. Mater.* **2000**, *12*, 646.
(12) Bartl, M. H.; Scott, B. J.; Huang, H. C.; Wirnsberger, G.; Popitsch, A.; Chmelka, B. F.; Stucky, G. D. *Chem. Commun.* **2002**, 2474.

(13) Bian, L.-J.; Qian, X.-F.; Yin, J.; Zhu, Z.-K.; Lu, Q.-H. *Mater. Sci. Eng.* **2003**, *B100*, 53.

(14) Guo, J. F.; Fu, L. S.; Li, H. R.; Zheng, Y. X.; Meng, Q. G.; Wang, S. B.; Liu, F. Y.; Wang, J.; Zhang, H. J. *Mater. Lett.* **2003**, *57*, 3899.

(15) Rosa, I. L. V.; Serra, O. A.; Nassar, E. J. *J. Lumin.* **1997**, *72*−*4*, 532.

(16) Xu, Q. H.; Fu, L. S.; Li, L. S.; Zhang, H. J.; Xu, R. R. *J. Mater. Chem.* **2000**, *10*, 2532.

(17) Xin, H.; Ma, R.; Wang, L. Z.; Ebina, Y.; Takada, K.; Sasaki, T. *Appl. Phys. Lett.* **2004**, *85*, 4187.

(18) Sasaki, T.; Watanabe, M.; Hashizume, H.; Yamada, H.; Nakazawa, H. *J. Am. Chem. Soc.* **1996**, *118*, 8329.

(19) Sasaki, T.; Watanabe, M. *J. Am. Chem. Soc.* **1998**, *120*, 4682.

(20) Melby, L. R.; Rose, N. J.; Abramson, E.; Caris, J. C. *J. Am. Chem. Soc.* **1964**, *86*, 5117.

(21) Sasaki, T.; Ebina, Y.; Tanaka, T.; Harada, M.; Watanabe, M.; Decher, G. *Chem. Mater.* **2001**, *13*, 4661.

(22) Hart, F. A.; Laming, F. P. *J. Inorg. Nucl. Chem.* **1964**, *26*, 579.

(23) Sasaki, T.; Watanabe, M. *J. Phys. Chem. B* **1997**, *101*, 10159.

(24) Sasaki, T.; Ebina, Y.; Kitami, Y.; Watanabe, M.; Oikawa, T. *J. Phys. Chem. B* **2001**, *105*, 6116.

(25) Sasaki, T.; Nakano, S.; Yamauchi, S.; Watanabe, M. *Chem. Mater.* **1997**, *9*, 602.

(26) Huang, C. H.; Li, F. Y.; Huang, Y. Y. *Ultra Thin Films for Optoelectronic Properties;* Peking University Press: Beijing, 2001.

(27) Xin, H.; Shi, M.; Gao, X. C.; Huang, Y. Y.; Gong, Z. L.; Nie, D. B.; Cao, H.; Bian, Z. Q.; Li, F. Y.; Huang, C. H. *J. Phys. Chem. B* **2004**, *108*, 10796.

(28) Malta, O. L.; Legendziewicz, J.; Huskowska, E.; Turowska-Tyrk, I.; Albuquerque, R. Q.; de Mello Donegá, C.; Silva, F. R. G. *J. Alloy. Compd.* **2001**, *323*, 654.

(29) Silva, F. R. G.; Menezes, J. F. S.; Rocha, G. B.; Alves, S.; Brito, H. F.; Longo, R. L.; Malta, O. L. *J. Alloy. Compd.* **2000**, *303*, 364.

(30) Gawryszewska, P.; Sokolnicki, J.; Dossing, A.; Riehl, J. P.; Muller, G.; Legendziewicz, J. *J. Phys. Chem. A* **2005**, *109*, 3858.

(31) Wu, R. H.; Zhao, H. Z.; Su, Q. *J. Non-Cryst. Solids* **2000**, *278*, 223.